Pergamon

Geochimica et Cosmochimica Acta, Vol. 66, No. 4, pp. 577–587, 2002

0016-7037/−1898 $22.00 + .00

PII S0016-7037(01)00816-X

The kinetics of oxygen exchange between the $GeO_4Al_{12}(OH)_{24}(OH_2)_{12}^{8+}$(aq) molecule and aqueous solutions

ALASDAIR P. LEE,[1] BRIAN L. PHILLIPS,[2,†] and WILLIAM H. CASEY,[1,3,*]

[1]Department of Land Air and Water Resources, Department of Geology, University of California, Davis, CA, USA
[2]Department of Chemical Engineering and Materials Science, University of California, Davis, CA, USA
[3]Department of Geology, University of California, Davis, CA, USA

(*Received June* 13, 2001; *accepted in revised form September* 17, 2001)

Abstract—We report rates of oxygen exchange with bulk solution for an aqueous complex, $^{IV}GeO_4Al_{12}(OH)_{24}(OH_2)_{12}^{8+}$(aq) ($GeAl_{12}$), that is similar in structure to both the $^{IV}AlO_4Al_{12}(OH)_{24}(OH_2)_{12}^{7+}$(aq) ($Al_{13}$) and $^{IV}GaO_4Al_{12}(OH)_{24}(OH_2)_{12}^{7+}$(aq) ($GaAl_{12}$) molecules studied previously. All of these molecules have ε-Keggin-like structures, but in the $GeAl_{12}$ molecule, occupancy of the central tetrahedral metal site by Ge(IV) results in a molecular charge of +8, rather than +7, as in the Al_{13} and $GaAl_{12}$. Rates of exchange between oxygen sites in this molecule and bulk solution were measured over a temperature range of 274.5 to 289.5 K and $2.95 < pH < 4.58$ using ^{17}O-NMR.

Apparent rate parameters for exchange of the bound water molecules (η-OH_2) are $k_{ex}^{298} = 200\ (\pm 100)\ s^{-1}$, $\Delta H^{\ddagger} = 46\ (\pm 8)$ kJ · mol^{-1}, and $\Delta S^{\ddagger} = -46\ (\pm 24)$ J · mol^{-1} K^{-1} and are similar to those we measured previously for the $GaAl_{12}$ and Al_{13} complexes. In contrast to the Al_{13} and $GaAl_{12}$ molecules, we observe a small but significant pH dependence on rates of solvolysis that is not yet fully constrained and that indicates a contribution from the partly deprotonated $GeAl_{12}$ species.

The two topologically distinct μ_2-OH sites in the $GeAl_{12}$ molecule exchange at greatly differing rates. The more labile set of μ_2-OH sites in the $GeAl_{12}$ molecule exchange at a rate that is faster than can be measured by the ^{17}O-NMR isotopic-equilibration technique. The second set of μ_2-OH sites have rate parameters of $k_{ex}^{298} = 6.6\ (\pm 0.2) \cdot 10^{-4}\ s^{-1}$, $\Delta H^{\ddagger} = 82\ (\pm 2)$ kJ · mol^{-1}, and $\Delta S^{\ddagger} = -29\ (\pm 7)$ J · mol^{-1} · K^{-1}, corresponding to exchanges ≈40 and ≈1550 times, respectively, more rapid than the less labile μ_2-OH sites in the Al_{13} and $GaAl_{12}$ molecules. We find evidence of nearly first-order pH dependence on the rate of exchange of this μ_2-OH site with bulk solution for the $GeAl_{12}$ molecule, which contrasts with Al_{13} and $GaAl_{12}$ molecules.

1. INTRODUCTION

Problems that interest Earth scientists are commonly difficult to approach experimentally, and there is an acute need for accurate methods of predicting reaction rates. For aqueous geochemists, the most important classes of reactions are those that break and form metal-oxygen bonds in water. One effective way to predict rate parameters is to identify key steps at a molecular scale that are common to a wide class of reactions and then correlate these rates to simple properties, such as bond lengths or Brønsted acidities, that vary systematically as well. Another approach is to simulate elementary steps in the reaction using *ab initio* electronic structure calculations and transition state theory.

In either case, the predictive model must be compared with experimental data at a very fundamental scale before it can be reliably applied to reactions in complicated geological settings. Furthermore, if transition state theory is employed, then the reactions must be *elementary*; that is, they must involve the motion of a few atoms in a single activated step. Ideally these fundamental data are needed at increasing scales of size and complexity, leading to simulations that can be applied to real geochemical problems, such as mineral growth and dissolution and adsorbate uptake and decomposition.

We are measuring the rates of exchange of oxygens between sites in multimeric cations of aluminum and bulk solution (e.g., Phillips et al., 2000; Casey and Phillips, 2001) with the goal of understanding <Al-O> bond dissociation at a fundamental level. The oxygen-exchange reactions described in these papers reflect bond-breaking processes at the *elementary* or near-*elementary* level that underlie more complex, multistep reactions, such as mineral dissolution. These reactions involve a few molecular motions and are therefore suitable for transition state theory. The molecules chosen for study contain structural sites that resemble those found in common aluminum (hydr)oxide mineral surfaces and are amenable to spectroscopic study. Of particular interest is the polyoxocation $AlO_4Al_{12}(OH)_{24}(H_2O)_{12}^{7+}$ (Al_{13}) because it exposes both bridging hydroxyl and terminal water groups to the bulk solution. In addition, single-atom substitutions can be made for the central ^{IV}Al to form, for example, the Ga(III) analog, $GaAl_{12}$, which is structurally similar to the Al_{13} molecule but differs considerably in oxygen exchange rates (Casey and Phillips, 2001). We have recently synthesized a Ge(IV)-substituted analog, $GeAl_{12}$ (Lee et al., 2001), and report here the reaction rates.

The Al_{13}, $GaAl_{12}$, and $GeAl_{12}$ molecules are isostructural and consist of a central tetrahedral $M(O)_4$ unit that is surrounded by 12 edge-sharing $Al(O)_6$ octahedra arranged in a structure similar to the Baker-Figgis ε-Keggin isomer (Fig. 1).

* Author to whom correspondence should be addressed (whcasey@ucdavis.edu).
† *Present address:* Geosciences Dept., State University of New York, Stony Brook, NY 11794-2100.

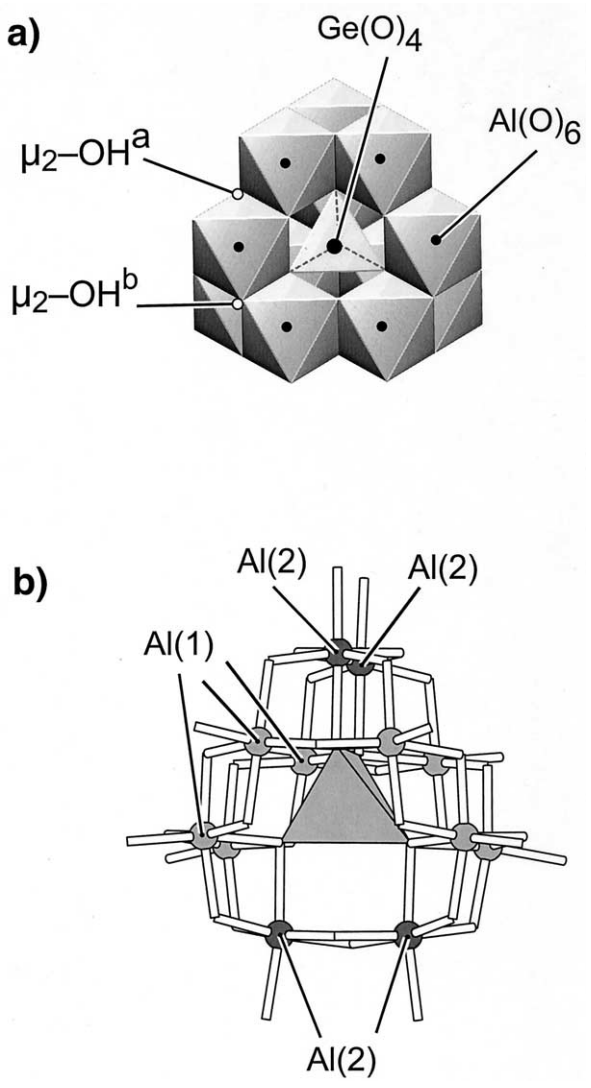

Fig. 1. (a) Polyhedral representation and (b) ball-and-stick model of the $GeO_4Al_{12}(OH)_{24}(H_2O)_{12}^{8+}$(aq) complex ($GeAl_{12}$). The molecule contains a tetrahedral GeO_4 unit surrounded by 12 AlO_6 octahedra. Each $GeAl_{12}$ unit contains 12 terminal water sites (η-OH_2) and two distinct sets of 12 shared μ_2-OH sites that are distinguished by their positions relative to the μ_4-O. The μ_2-OH^a site (a) is *cis* to two μ_4-O, and the μ_2-OH^b is *cis* to one μ_4-O sites. For the $GeAl_{12}$ molecule, each of these two sets is split into two crystallographically distinct positions by a tetrahedral distortion caused by the introduction of the more highly charged Ge(IV) ion. The ball-and-stick model (b) identifies distinct aluminum sites (Al_1 and Al_2) created by the distortion (Lee et al., 2001).

Both the $GaAl_{12}$ and Al_{13} cations exhibit cubic symmetry within their respective selenate and sulfate salts and have 12 equivalent bonded water molecules (η-OH_2), two structurally distinct sets of 12 hydroxyl bridges (μ_2-OH^a; μ_2-OH^b), and one set of 4 equivalent four-coordinated oxo groups (μ_4-O). Of these oxygen sites, only the μ_4-O groups are inert with respect to exchange with the bulk solution. The ^{IV}Ge(IV) ion can be substituted for ^{IV}Al(III) in the Al_{13} structure because these two ions have the same ionic radius (0.53 nm; Cotton et al., 1999), even though they differ in charge.

Substitution of Ge(IV) for Al(III) causes a slight tetragonal distortion from the cubic symmetry exhibited by the Al_{13} and $GaAl_{12}$ molecules in their selenate and sulfate salts. The Al_{13} and $GaAl_{12}$ ε-Keggin-like molecules each have octahedral aluminums in equivalent sites surrounding the central tetrahedral metal. Substitution of ^{IV}Ge(IV) into the central position produces a slight differential expansion in the axial and equatorial directions that produces two distinct sets of octahedral aluminum sites in the $GeAl_{12}$ molecule in crystals: the axial Al(2) positions with multiplicity of four and the equatorial Al(1) positions with multiplicity of eight (Fig. 1b). The cubic Al_{13} and $GaAl_{12}$ molecules contain only four distinct oxygen positions, corresponding to the η-OH_2, μ_4-O, and the topologically distinct μ_2-OH^a and μ_2-OH^b. The symmetry reduction upon ^{IV}Ge(IV) for ^{IV}Al(III) substitution splits each of the two topologically distinct sets of μ_2-OH and the η-OH_2 into two crystallographic positions, but not the μ_4-oxo sites. These distortions are apparent in single-crystal X-ray structures and the solid-state NMR spectra of the $GeAl_{12}$ selenate salt (Lee et al., 2001) but are not observed in the solution-state ^{27}Al or ^{17}O-NMR spectra presented below. The distortions are slight relative to the topological differences between the μ_2-OH^a and μ_2-OH^b sites shown in Figure 1a and are probably dynamically averaged for the dissolved molecule on the NMR time scale.

2. MATERIALS AND METHODS

2.1. Synthesis of $GeAl_{12}$ Salts and Preparation of Solutions

The $GeAl_{12}$ polyoxocation was synthesized by the titration of a 300-mL volume of 0.26 mol/L $AlCl_3$ solution against 178 mL of 1.125 mol/L NaOH solution containing 0.058 mol of GeO_2 at 85°C. The resulting solution was filtered hot and then quenched in deionized water before adding 0.2 mol/L $Na_2SeO_4(H_2O)_{10}$ solution to give an 8:1 SeO_4 excess. The resulting solution was then diluted to a total volume of 1200 mL with cold 18 MΩ water. Colorless tetrahedral crystals of $GeO_4Al_{12}(OH)_{24}(H_2O)_{12}(SeO_4)_4(H_2O)_x$ ($x \approx 10$) form after ~1 week and were harvested after 10 d. All batches were characterized by single-crystal X-ray diffraction and solid-state ^{27}Al-NMR and were found to contain less than 1% impurity Al_{13}. A full description of this new polyoxocation is given elsewhere (Lee et al., 2001).

The solution-state NMR experiments were conducted on samples extracted from the $GeAl_{12}$ selenate salt according to the methods established by Phillips et al. (2000) and Casey et al. (2000). Accurately weighed samples of ~0.067 g (3.5×10^{-4} mol) of $GeAl_{12}$ crystals were ground with ~0.14 g (5.5×10^{-4} mol) of $BaCl_2(H_2O)_2$, after which 2 mL of isotopically normal water were added and the mixture shaken vigorously for 10 min. The extracted solution of $GeAl_{12}$ was separated from the barium-selenate precipitate by aspiration through a 0.2-μm filter. This extracted solution and a sample of 36% ^{17}O-enriched water (Isotec Laboratories) that was 0.5 mol/L in manganous chloride were separately thermally equilibrated at the desired temperature. At a precisely determined time t_o, 1 mL of the ^{17}O-labeled Mn(II) solution was added rapidly to 1 mL $GeAl_{12}$ filtrate in a thermally equilibrated glass cell that allowed for immediate measurement of pH, then transferred into a thermally equilibrated NMR tube and introduced into the spectrometer. Typically, the time between introduction of the

Table 1. Experimental results.

(**a**) Exchange of μ_2-OH sites; τ_1 is too short to measure.

Sample	T (K)	$pH_{initial}$	pH_{final}/[a] (h)	τ_2 (s) ($\pm 1\sigma$)
H56	282.5	4.85		10,500 ($\pm$500)
H53	278.8	4.92		Not measured
H44	288	4.68		5100 ($\pm$300)
H62	297	4.53		1580 ($\pm$80)
H65	303	4.6		950 ($\pm$60)
H68b	292.5	4.48		2400 ($\pm$100)
H70c	292.5	4.22		1700 ($\pm$100)
H74	292.5	3.95		990 ($\pm$70)
H75	292.5	4.12	4.19/2 h	1350 ($\pm$80)
H76b	292.5	4.11	4.11/2 h	2100 ($\pm$100)
H94	335.5	3.63	2.96	

[a] Elapsed time between pH measurements.

(**b**) Exchange of the η-OH_2 sites.

Sample	k_{ex}^{298} (s^{-1})	$\Delta H^{\ddagger}$ ($kJ \cdot mol^{-1}$)	$\Delta S^{\ddagger}$ ($J \cdot K^{-1} \cdot mol^{-1}$)	$W_{q,298}$ (s^{-1})	E_q ($kJ \cdot mol^{-1}$)
3259	191 ($\pm$80)	46 ($\pm$8)	–48 ($\pm$24)	1030 ($\pm$95)	21 ($\pm$3)
H44	340 ($\pm$90)	34 ($\pm$5)	–81 ($\pm$14)	800 ($\pm$100)	25 ($\pm$4)
H48	180 ($\pm$60)	46 ($\pm$7)	–46 ($\pm$22)	970 ($\pm$80)	23 ($\pm$3)
H56a	210 ($\pm$60)	48 ($\pm$6)	–39 ($\pm$14)	—	
All data	200 ($\pm$100)	46 ($\pm$8)	–46 ($\pm$24)	1027 ($\pm$88)	21 ($\pm$3)

isotopically enriched water and the conclusion of the first NMR experiment was 5 min or less.

A parallel set of experiments in isotopically normal water was run to determine the acid needed to reach a target pH value and the drift in the solution pH with time. From this series, samples H70-H76 were made by adding 0.1 mol/L HCl to the 0.5 mol/L $MnCl_2$ solution containing ^{17}O-enriched water.

2.2. Temperature Control

Temperature stability and accuracy of settings were determined by the same method used in our previous studies of Al_{13} and $GaAl_{12}$ (Casey et al., 2000; Casey and Phillips, 2001). Stability of the spectrometer temperature controller and water bath was better than $\pm$0.2 K, but as in our previous studies of Al_{13} and $GaAl_{12}$, we employed a more conservative $\pm$0.5 K standard deviation for temperature variation to calculate rate coefficients. Temperatures were measured with a Cu-constantan thermocouple located in the center of a sample assembly identical to that used for the NMR experiments.

2.3. pH and Solution Chemistry

The pH of the $GeAl_{12}$ solutions stabilizes quickly after extraction. This stability is due to partial dissociation of the molecule and self-buffering of the solution pH; however, the pH value of this extracted solution varies significantly with temperature (Table 1a), indicating that the molecule is more dissociated at higher temperature than at room temperature. The pH of an unacidified sample does not drift significantly over the length of the NMR experiments, typically 4 to 10 h. Acidified solutions slowly equilibrated back to original solution pH. This pH drift limits the conditions accessible for measurement of the pH dependence of exchange rates for oxygens in μ_2-OH sites. Therefore we conducted these experiments at higher temperatures, at which isotopic equilibration is complete before the pH drifted.

We collected ^{27}Al-NMR spectra before and after experiments to monitor the extent to which the molecule dissolved over the lifetime of the ^{17}O-NMR experiment. In most cases, the concentration of monomeric aluminum released by hydrolysis of the $GeAl_{12}$ was negligible. An exception was sample H74 (Table 1), in which the solution was acidified to pH = 3.95, which was the lowest pH value used in the rate study. In this sample, 41% of the $GeAl_{12}$ molecule decomposed to release aluminum monomers during the rate measurement.

The solution pH was determined using a combination electrode at temperature that had been calibrated on the concentration scale. Calibration was accomplished by titrating standard solutions containing 0.25 mol/L $BaCl_2$ and 0.25 mol/L $MnCl_2$ against 0.100 mol/L hydrochloric acid, also at temperature. The apparent ionic strength of each solution is $\sim$1.7. To make this calculation we assume that the molecular weight of the $Na[GeO_4Al_{12}(OH)_{24}(H_2O)_{12}(SeO_4)_4](H_2O)_x$ crystals dissolved into the aqueous solution is 1813 g mol^{-1}. There can be small deviation from this value depending upon the hydration state of the salt.

2.4. NMR Spectroscopy

Solution-state ^{17}O and ^{27}Al-NMR experiments were conducted using a 10-mm broadband probe on a Bruker Avance spectrometer based on an 11.7-T magnet and operating at 67.8 MHz for ^{17}O and 130.3 MHz for ^{27}Al. The ^{17}O-NMR spectra were measured with single-pulse excitation of 20 μs ($\pi/2$ pulse $\approx$ 40 μs) with a recycle delay of 6 ms. Depending upon temperature, between 10,000 and 40,000 acquisitions were required to achieve an adequate signal-to-noise ratio yet still allow adequate time resolution. Time domain data were digi-

tized at 100 kHz, and baselines were corrected by recalculating the first seven points by a linear prediction algorithm before Fourier transformation (Cavanagh et al., 1996). The ^{27}Al-NMR spectra were measured under broadly similar conditions (see Casey et al., 2000) but with recycle delays of 1 s and typically no more than 256 acquisitions. Quantitative ^{27}Al-NMR experiments indicate that no significant dissolution of the $GeAl_{12}$ complex occurred during the longest experiments on unacidified samples.

In common with our previous studies (e.g., Phillips et al., 2000; Casey and Phillips, 2001), we included a coaxial insert of isotopically normal 0.3 mol/L $TbCl_3$ as an intensity standard in the ^{17}O-NMR experiments. This insert gives a peak at ~ -100 ppm that corresponds to bulk waters and waters of hydration on the Tb(III) ion that are in rapid-exchange equilibrium. The intensity of this peak represents a constant number of ^{17}O nuclei, allowing changes in the absolute ^{17}O-NMR intensities from the $GeAl_{12}$ molecule to be determined. Line shape parameters were determined for all peaks in the ^{17}O-NMR spectrum from least squares fits of the frequency domain data to a sum of Lorentzian curves. Conservatively estimated uncertainties of 10% in the raw line width and 0.02 in relative intensity (total intensity normalized to unity) were propagated through the calculations of rate parameters using Monte Carlo techniques.

3. RESULTS

3.1. ^{17}O-NMR Peak Assignments

The essential features of the ^{17}O-NMR spectra for the $GeAl_{12}$ complex (Fig. 2) closely resemble those for the structurally similar Al_{13} and $GaAl_{12}$ molecules (see Phillips et al., 2000). The spectrum exhibits a relatively narrow peak near -100 ppm that corresponds to the aqueous $TbCl_3$ coaxial insert. Downfield of the standard peak at -100 ppm is another relatively narrow peak near 22 ppm that exhibits near-constant intensity relative to the standard. On the basis of our previous work (e.g., Phillips et al., 2000), this peak at 22 ppm is assigned to the η-OH_2 groups in the $GeAl_{12}$ complex. These bound water molecules are isotopically equilibrated with the solution in fractions of a second (see below). Throughout the course of an experiment, the intensity ratio of these peaks at 22 and -100 ppm varies by less than a few percent.

Further downfield from the peak at 22 ppm is a broad shoulder that is centered near 35 ppm. The intensity of this peak at 35 ppm increases with time, as we observed previously for similar experiments on $GaAl_{12}$ and Al_{13} molecules; however, unlike the previous studies, the shoulder is observed in the very first spectrum at temperatures where it is narrow enough to be observed easily (Fig. 2). The peak intensity increases with time to asymptotically approach a constant value at rates that vary with temperature and solution pH. The peak near 35 ppm is a sum of contributions from the two structurally distinct μ_2-OH sites in the molecule, for reasons detailed below and by Phillips et al. (2000).

3.2. Rates of Exchange of Bound and Bulk Water Molecules

The methods of determining rate coefficients were presented by Phillips et al. (2000) and will not be reviewed extensively here. Briefly, the rates of exchange with bulk solution of water molecules bound to the $GeAl_{12}$ ion were determined via the dynamic ^{17}O line-broadening technique (Swift and Connick, 1962). Transverse relaxation times (T_2) may be measured directly from the line width of the NMR spectrum by the relationship $T_2 = 1/\pi \cdot FWHM$ where FWHM is the full width at half maximum of the ^{17}O-NMR peak at 22 ppm obtained from least squares fits of the spectra. The signal from bulk water was eliminated by the addition of Mn(II) into the solution, which forms aqueous complexes that broaden this peak beyond detection under the experimental conditions used here (Hugi-Cleary et al., 1985).

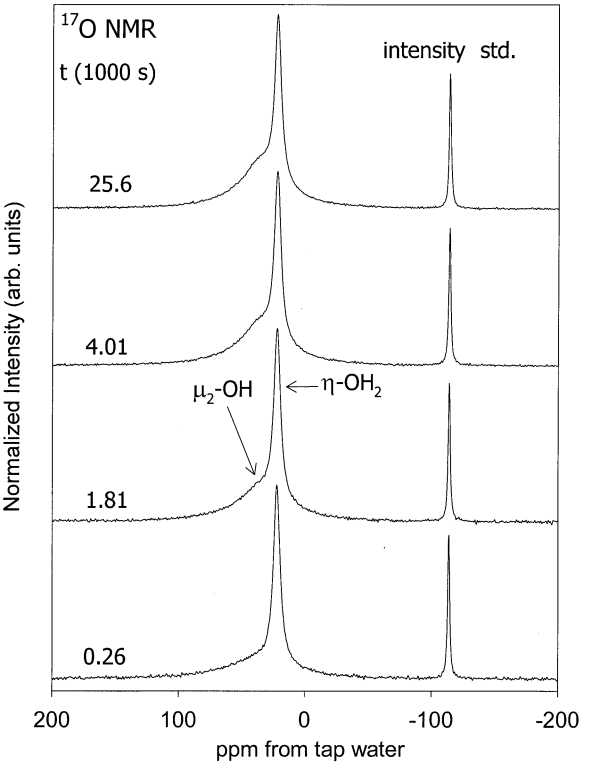

Fig. 2. ^{17}O nuclear magnetic resonance spectra as a function of time for sample H68b, temperature = 292.5 K. Intensities are normalized to the peak at -120 ppm that arises from the external Tb^{3+}(aq) intensity standard.

Two processes with opposite temperature dependencies control the ^{17}O-NMR line widths of the bound water molecules. At low temperatures, quadrupolar relaxation dominates T_2 relaxation and causes line widths to decrease as temperature increases from 274 to $\sim$304 K. The line widths reach a minimum near 304 K (Fig. 3) and increase with temperature thereafter as chemical exchange of bound and bulk waters becomes increasingly important to T_2 relaxation.

The net rates of ^{17}O-NMR transverse relaxation ($1/T_2$) contain contributions from both of these relaxation mechanisms:

$$\frac{1}{T_2} = \frac{1}{\tau} + \frac{1}{T_{2,q}}, \tag{1}$$

where τ is the mean lifetime of a water molecule in the inner coordination sphere, and $1/T_{2,q}$ is the intrinsic quadrupolar

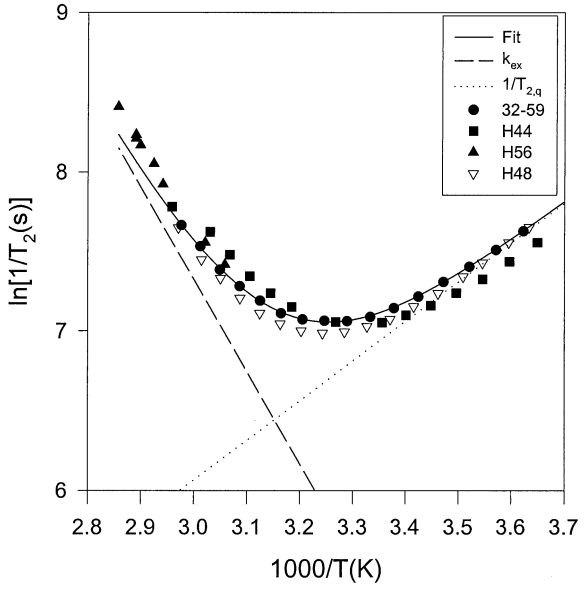

Fig. 3. Values of $\ln(1/T_2)$ as a function of temperature for the bound waters (η-OH_2) of $GeAl_{12}$. Eqn. 1 to 3 were fit to these data to derive the rates of exchange of bound waters from sites in the $GeAl_{12}$ complex to bulk solution. Different symbols correspond to different samples in Table 1. Values of $1/T_2$ are obtained from the width of the peak at 22 ppm returned from an unconstrained least squares fit of the spectra to a sum of Lorentzian curves. The dotted line is the contribution to the line width from quadrupolar relaxation (Eqn. 2), and the dashed line is the contribution from chemical exchange (Eqn. 3) in the least squares fit.

relaxation rate. The rates for quadrupolar relaxation are approximated using an Arrhenius function:

$$\frac{1}{T_{2,q}} = W_{q,298} e^{\frac{E_q}{R}\left[\frac{1}{T}-\frac{1}{298}\right]}, \qquad (2)$$

where E_q and $W_{q,298}$ are fitting parameters.

The temperature dependence of $k_{ex}(s^{-1})$, the first-order rate coefficient for exchange of water molecules from the inner coordination sphere to the bulk solution, takes the form of the Eyring equation:

$$k_{ex} = \frac{1}{\tau} = \frac{k_b \cdot T}{h} e^{\frac{\Delta S^{\neq}}{R}} e^{\frac{\Delta H^{\neq}}{R \cdot T}}, \qquad (3)$$

where k_b is Boltzmann's constant, and the exponential terms include the activation entropy ($\Delta S^{\ddagger}$) and activation enthalpy ($\Delta H^{\ddagger}$) for chemical exchange. The parameters T, R, and h are absolute temperature, the gas constant, and Planck's constant, respectively. The results of least squares fits of Eqn. 1 to 3 to the data are given in Table 1b, and a fit to all of the data is presented graphically in Figure 3.

The T_2 values were measured as a function of temperature for four samples that had been isotopically equilibrated during an OH-exchange measurement (Fig. 3). These data yield an apparent pseudo-first-order exchange rate coefficient of $\approx$175 s^{-1} at 298 K (Table 2), which is similar to those measured for the Al_{13} and $GaAl_{12}$ complexes of 1100 and 227 s^{-1}, respectively (see Phillips et al., 2000; Casey and Phillips, 2001).

However, these results show much more scatter than previous measurements for $GaAl_{12}$ and Al_{13}, which would indicate a contribution from a pH-dependent process. This hypothesis is supported by changes in the width of the peak near 22 ppm upon addition of small amounts of acid at temperatures at which the peak width is dominated by chemical exchange effects (Fig. 4). For these experiments, $GeAl_{12}$ was extracted directly into $\approx$15% ^{17}O-enriched water, which yielded widths that varied from 800 to 1000 Hz, depending on the sample (Fig. 4a). Upon addition of small amounts of acid, the width decreased to 420 $\pm$ 20 Hz (62°C) and did not change with further acid addition (Figs. 4a and 4b). This result suggests that the 420-Hz value corresponds to the contribution from the pH-independent path. After acidification, a peak near 76 ppm appears gradually (Fig. 4c) that can be tentatively assigned to the μ_4-O groups (Thompson et al., 1987), suggesting that the $GeAl_{12}$ is dissociating and reforming at this pH of 2.96.

The pH dependence arises from the presence at higher pH of a partially deprotonated $GeAl_{12}$ species, which probably exhibits much faster water exchange rates than the fully protonated

Table 2. A compilation of rate coefficients and activation parameters for exchange of water molecules from the inner-coordination sphere of Al(III) complexes to the bulk solution, as determined from ^{17}O nuclear magnetic resonance.

Species	k_{ex}^{298} (s^{-1}) ($\pm 1\sigma$)	$\Delta H^{\ddagger}$ ($kJ \cdot mol^{-1}$)	$\Delta S\ddagger$ ($J \cdot K^{-1} \cdot mol^{-1}$)	Source
Monomeric complexes				
$Al(H_2O)_6^{+3}$	1.29 ($\pm$.03)	85 ($\pm$3)	42 ($\pm$9)	Hugi-Cleary et al. (1985)
$Al(H_2O)_5OH^{2+}$	31,000 ($\pm$7750)	36 ($\pm$5)	–36 ($\pm$15)	Nordin et al. (1999)
$AlF(H_2O)_5^{2+}$	240 ($\pm$34)	79 ($\pm$3)	17 ($\pm$10)	Yu et al. (2001)
$AlF_2(H_2O)_4^{+}$	16,500 ($\pm$980)	65 ($\pm$2)	53 ($\pm$6)	Yu et al. (2001)
$Al(ssal)^{+}$	3000 ($\pm$240)	37 ($\pm$3)	–54 ($\pm$9)	Sullivan et al. (1999)
$Al(sal)^{+}$	4900 ($\pm$340)	35 ($\pm$3)	–57 ($\pm$11)	Sullivan et al. (1999)
$Al(mMal)^{+}$	660 ($\pm$120)	66 ($\pm$1)	31 ($\pm$2)	Casey et al. (1998)
$Al(mMal)_2$–	6900 ($\pm$140)	55 ($\pm$3)	13 ($\pm$11)	Casey et al. (1998)
$Al(ox)^{+}$	109 ($\pm$14)	69 ($\pm$2)	25 ($\pm$7)	Phillips et al. (1997b)
Multimeric complexes				
Al_{13}	1100 ($\pm$100)	53 ($\pm$12)	–7 ($\pm$25)	Phillips et al. (2000), Casey et al. (2001)
$GaAl_{12}$	227 ($\pm$43)	63 ($\pm$7)	29 ($\pm$21)	Casey and Phillips (2001)
$GeAl_{12}$	190 ($\pm$43)	56 ($\pm$7)	20 ($\pm$21)	This paper

Abbreviations: ox = oxalate; ssal = sulfosalicylate; sal = salicylate; mMal = methylmalonate; $Al_{13} = AlO_4Al_{12}(OH)_{24}(H_2O)_{12}^{7+}$(aq); $GaAl_{12} = GaO_4Al_{12}(OH)_{24}(H_2O)_{12}^{7+}$(aq); and $GeAl_{12} = GeO_4Al_{12}(OH)_{24}(H_2O)_{12}^{8+}$(aq).

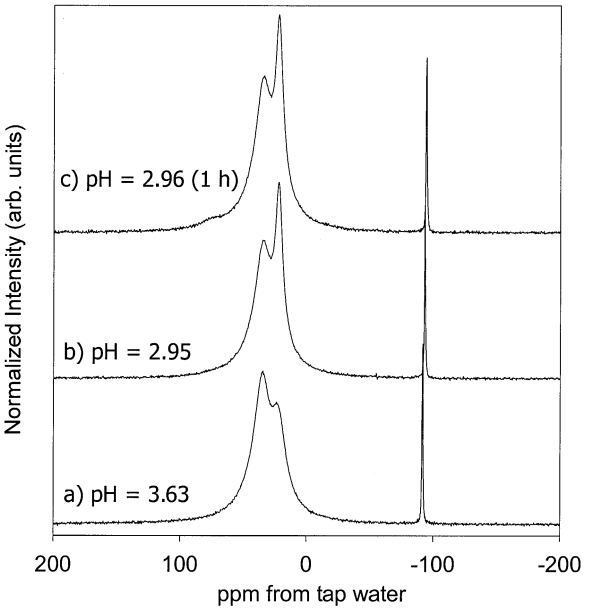

Fig. 4. ^{17}O nuclear magnetic resonance spectra of sample H94 at a temperature of 335.5 K (a) as extracted, (b) immediately after addition of acid, and (c) 1 h after acid addition. Spectra are scaled to constant intensity for the external standard near $\delta = -95$ ppm. Frequencies are referenced to the hydration waters at 22 ppm.

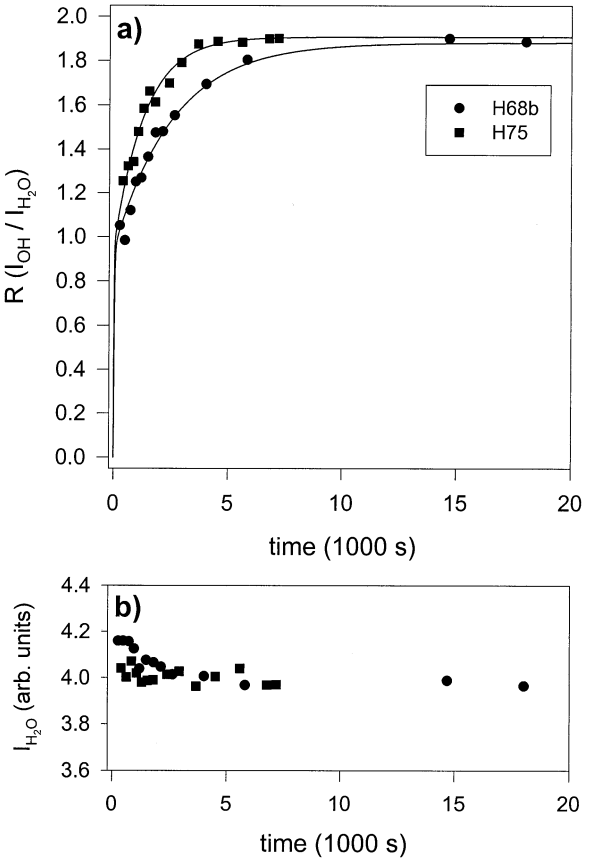

Fig. 5. (a) The intensity ratio $R(t) = I_{\delta=35}/I_{\delta=22}$ as a function of time after adding $H_2^{17}O$ to the extracted solution at 292.5 K. $R(t) \approx 1.0$ for the very first spectrum ($t \approx 300$ s), indicating that the more reactive of the two μ_2-OH sites isotopically equilibrated with bulk solution by this time. The rate at which $R(t) \rightarrow 2.0$ varies with pH and temperature. Data are shown for two pH conditions: sample H68b (pH = 4.48, τ_2 = 2400 ($\pm$100) s) and sample H75 (4.12 < pH < 4.19, τ_2 = 1350 ($\pm$80) s; Table 1). The $\tau_1 < 60$ s at this temperature. (b) For the same two samples, the ratio of the intensity of the peak at 22 ppm, assigned to the bound waters, relative to the peak that corresponds to the external standard solution. The values are constant to within experimental error.

complex (e.g., Nordin et al., 1998). Further investigation of this aspect requires measurement of the Brønsted acidity of this complex. By analogy with the Al_{13} molecule, the dissociation probably occurs in the range $5.5 < pH < 6.5$ (Furrer et al., 1992), although the pH dependence of exchange rate may indicate that the $GeAl_{12}$ molecule is a somewhat stronger acid than either the Al_{13} or $GaAl_{12}$ molecules, for which no pH dependence was observed. Regardless, the k_{ex} value given by the present data is likely to be within a factor of two of the exchange coefficient for the fully protonated $GeAl_{12}$ complex, since the variation in line width with pH is small.

3.3. Oxygen Exchange between Bulk Solution and μ_2-OH Sites

As we observed for the Al_{13} and $GaAl_{12}$ molecules, the rate of increase in ^{17}O-NMR intensity for the 35 ppm peak provides evidence for two kinetically distinct time scales for oxygen exchange at the μ_2-OH sites. The two time scales are evident in the plots of the ratio of intensities for the peak at 35 ppm relative to that for the peak at 22 ppm, which exhibits approximately constant intensity as a function of time and is assigned to the bound water molecules (η-OH_2) in the complex. Briefly, we define the ratio of peak intensities: $R(t) = I_{\delta=35}/I_{\delta=22}$, where t is the time elapsed since addition of the ^{17}O-enriched water, and $I_{\delta=35}$ and $I_{\delta=22}$ are the integrals of the single Lorentzian curve fit to the peak near $\delta = 35$ ppm and $\delta = 22$ ppm, respectively (Fig. 5a).

For $GeAl_{12}$ solutions, the time constant for exchange of the more labile μ_2-OH site could not be measured with the current techniques because $R(t) \approx 1$ in the very first ^{17}O-NMR spectrum ($t \approx 300$ s) in the temperature range of 274 to 303 K. In the temperature range 278.8 to 303 K, $R(t)$ increases from $R(t) \approx 1$ to asymptotically approach $R(t) = 2$ at a rate that is sufficiently slow to measure (Fig. 5). (Please note that τ_1 and τ_2 denote the characteristic times for exchange of the hydroxyl bridges, which were determined by the isotope-equilibration method, not by the ^{17}O-NMR line-broadening method and Eqn. 1. to 3.).

In experiments with the Al_{13} and $GaAl_{12}$ molecules, the ratio of intensities reached a value of $R(t) = 2.0$ upon isotopic equilibration, consistent with the stoichiometry of these molecules, as they each contain two distinct sets of 12 μ_2-OH sites (24 total) and 12 bound water molecules. For the $GeAl_{12}$ molecule, least squares fits to the spectra of isotopically equilibrated samples yielded R values somewhat less than 2 ($1.8 < R < 2.0$) and remained constant thereafter. Deviation of R from 2.0 upon isotopic equilibration does not indicate a change in the reaction stoichiometry but is likely an artifact of the NMR data reduction process that makes it difficult to measure the intensity of broad peaks. Corruption of the initial data points

in the time domain causes baseline distortion that becomes increasingly difficult to distinguish from intensity for broad peaks, which also decays quickly in the time domain. The NMR peaks corresponding to the μ_2-OH sites in the $GeAl_{12}$ molecule are significantly broader relative to those in the Al_{13} and $GaAl_{12}$. For example, at equilibrium and 301 K, the widths for peaks assigned to the rapidly and slowly exchanging μ_2-OH sites in the $GaAl_{12}$ molecule were 2700 and 1600 Hz, respectively, whereas the corresponding peaks from $GeAl_{12}$ are 3200 and 2000 Hz. The value $R(t) = 1.8$ is within experimental error of $R(t) = 2.0$, corresponding to a difference of ≈2% in the relative intensities of the peaks at $\delta =$ 35 ppm and $\delta = 22$ ppm.

As was observed for the Al_{13} and $GaAl_{12}$ molecules (see Phillips et al., 2000), these data indicate that the rate of isotopic equilibration for the peak at 35 ppm has contributions from two reactions: one fast and the other relatively slow. From these arguments, we assign the peak at 35 ppm to the two structurally distinct but spectroscopically unresolved μ_2-OH sites in the $GeAl_{12}$ molecule. Structurally, one site (μ_2-OH^a) is *cis* to two μ_4-O sites, and the other site (μ_2-OH^b) is *cis* to a single μ_4-O in the $GeAl_{12}$ molecule (Fig. 1; Lee et al., 2001).

The simplest explanation of these data is that the two time scales correspond to oxygen exchange into μ_2-OH^a and μ_2-OH^b and that one of these sites isotopically equilibrates before a single spectrum can be collected. Although the crystal structure of the $GeAl_{12}$ selenate salt indicates that there are two crystallographically distinct positions for both the μ_2-OH^a- and μ_2-OH^b-type sites, the distortions from cubic symmetry are small compared to the topological difference between the μ_2-OH^a and μ_2-OH^b sites. Furthermore, we expect that the tetragonal distortion would be dynamically averaged in the solution state on a time scale much shorter than that for the oxygen exchange.

With these peak assignments, the experimental $R(t)$ values were fit to a rate law that is a sum of two exponential terms:

$$R(t) = \frac{I_{\delta=35}(t)}{I_{\delta=22}} = C - e^{-\frac{t}{\tau_1}} - e^{-\frac{t}{\tau_2}}, \quad (4)$$

where t is the elapsed time since the addition of ^{17}O to an extracted solution of $GeAl_{12}$ complex, τ_1 and τ_2 are the characteristic times for exchange, and $C = 2$ from the stoichiometry of the complex. Note that $I_{\delta\,=\,22}$ is assigned to the bound water molecules, and $I_{\delta\,=\,35}$ corresponds to the intensities the sum of μ_2-OH^a + μ_2-OH^b sites. Eqn. 4 is a form of the McKay equation for isotopic equilibration kinetics, and numerical values for the first-order rate coefficients for chemical exchange at the two sites can be derived directly: $k_i = 1/\tau_i$ (see Casey et al., 2000). In the present case, τ_1 is much shorter than τ_2 and could not be measured. The value of C was allowed to vary to compensate for systematic errors in the fitted intensity of the peak at $\delta = 35$ ppm, reducing Eqn. 4 to

$$R(t) = [C - 1.0] - e^{-\frac{t}{\tau_2}}. \quad (5)$$

Typical fits of Eqn. 5 to the data are shown in Figure 5.

The fact that we could not measure a rate for the more reactive component distinguishes the present results for the $GeAl_{12}$ molecule from those of the Al_{13} and $GaAl_{12}$ molecules, for which values of both τ_1 and τ_2 were obtained. However, all of the spectral changes that occur as a function of time can be attributed to an exponential increase in the intensity of a second component at 35 ppm, corresponding to characteristic time τ_2. Results from experiments at all temperatures are compiled in Table 1a.

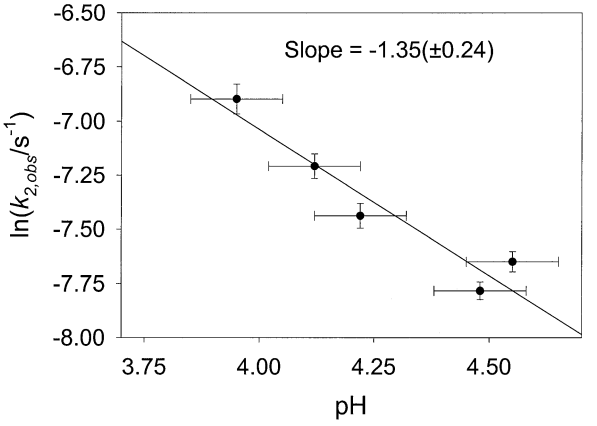

Fig. 6. Variation in the observed exchange rate at 292.5 K for the less labile hydroxyl ($k_{2,obs} = 1/\tau_2$) as a function of proton concentration. The uncertainties correspond to a single estimated standard deviation.

3.4. Variation of Rates with Proton Concentration

In our studies of oxygen exchange in the Al_{13} and $GaAl_{12}$ molecules we found no evidence for a dependence of τ_1 or τ_2 values with pH. Although the experimentally accessible pH range was relatively narrow, a first-order dependence of oxygen exchange rate on proton concentration could be ruled out for both the $GaAl_{12}$ and Al_{13}. For the $GeAl_{12}$ molecule, however, we see clear evidence of a strong pH dependence on the exchange rate (Fig. 6) that is close to first order in dissolved proton concentration.

The slope of the regression shown in Figure 6 is −1.35 (±0.24) and is probably indistinguishable from first-order dependence on proton concentration given the very narrow range in accessible pH and the relatively large experimental uncertainties. The range of pH accessible to study in this molecule is limited to ~0.5 pH units. Acidification beyond pH = 3.9 causes changes in the ^{17}O-NMR spectra from proton-enhanced decomposition of $GeAl_{12}$ molecules that are difficult to distinguish from those due to isotopic equilibration reactions. This decomposition appears to occur much more rapidly in the $GeAl_{12}$ than in either the Al_{13} or $GaAl_{12}$ complexes.

3.5. Variation with Temperature

The values of $k_{2,obs} = 1/\tau_2$ vary exponentially with temperature (Fig. 7). Application of the Arrhenius rate law to the temperature variation yields apparent activation parameters of $\Delta H^{\ddagger} = 82$ (±2) kJ · mol^{-1} and $\Delta S^{\ddagger} = -29$ (±7) J · mol^{-1} · K^{-1}. The temperature dependence is compared with data for

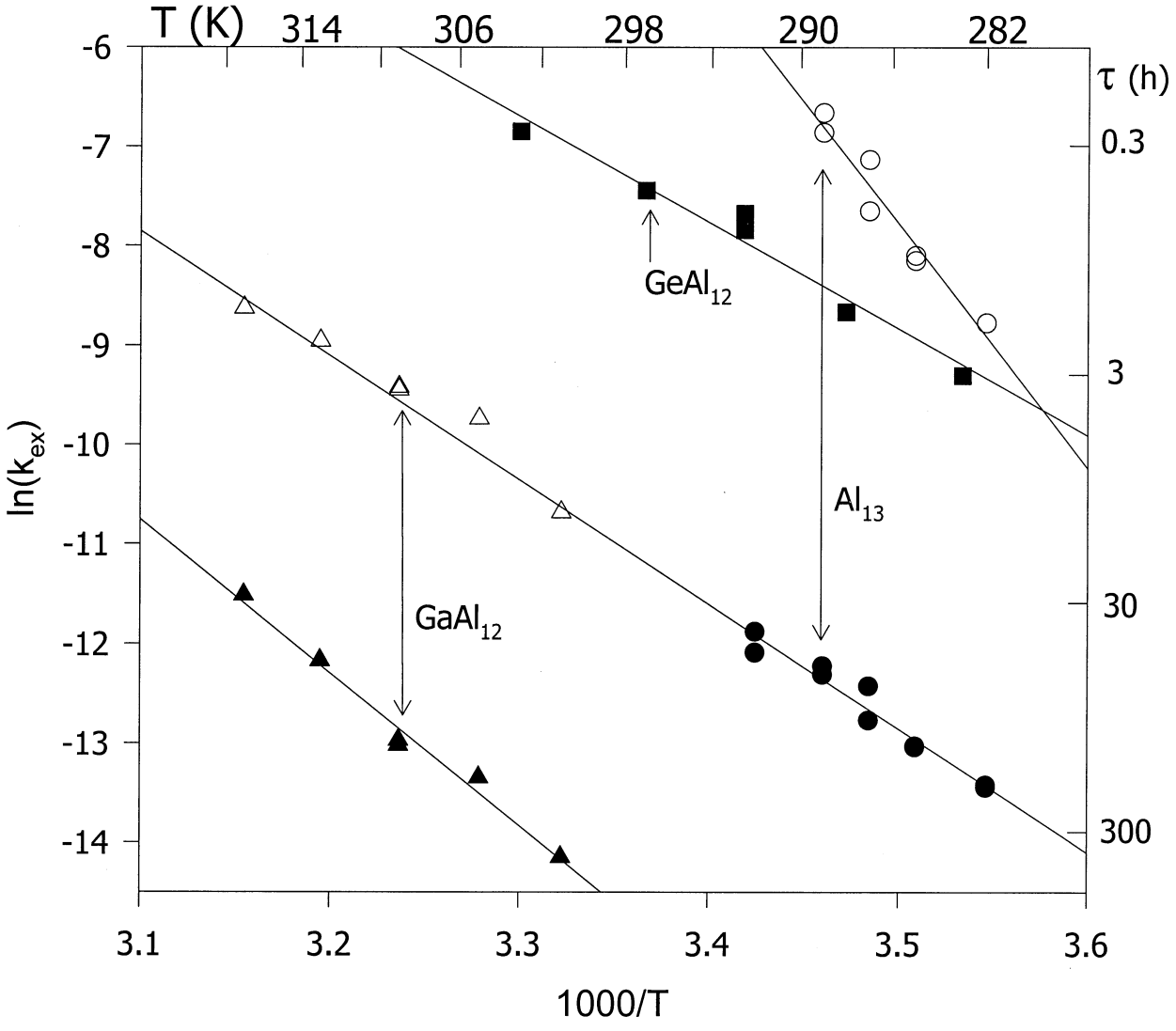

Fig. 7. Arrhenius plot of the observed oxygen exchange rates and average lifetimes (τ_i, right-hand side) for the μ_2-OH sites in the Al_{13}, $GaAl_{12}$, and $GeAl_{12}$. The open and closed symbols correspond to fast- and slow-reacting μ_2-OH sites in the same molecule. Arrows link the values of τ_1 and τ_2 corresponding to each molecule. There is no value of τ_1 for the $GeAl_{12}$ because the rates are too fast to measure. Note that the slope of the values of τ_2 for the $GeAl_{12}$ are significantly different than for τ_2 in either the Al_{13} or $GaAl_{12}$ molecules.

the Al_{13} and $GaAl_{12}$ molecules in Figure 7. The $\Delta H^{\ddagger}$ value for exchange of the μ_2-OH site in the $GeAl_{12}$ molecule is smaller than $\Delta H^{\ddagger}$ values for either site in the Al_{12} (202 and 104 kJ · mol^{-1}) or the $GaAl_{12}$ molecules (98 and 125 kJ · mol^{-1}). The smaller activation energy likely results from a contribution from the enthalpy of protonating the bridging hydroxyls, as we discuss in the next section.

4. DISCUSSION

4.1. Activation Energies

In contrast to the Al_{13} and $GaAl_{12}$ molecules, the rates of exchange of both the bound waters and the μ_2-OH site for the $GeAl_{12}$ vary with pH. As with the $GaAl_{12}$ and Al_{13} molecules, we cannot assign the values of τ_1 or τ_2 to μ_2-OH^a or μ_2-OH^b sites in the molecule, although it is clear that these two sites react at dramatically different rates. By analogy with OH exchange for hydroxy-bridged dimers and other larger polyoxocations (e.g., Springborg, 1988), there are probably two pathways for exchange of a single μ_2-OH site, of which both contribute significantly to the rate coefficient ($k_{2,obs} = 1/\tau_2$) observed for $GeAl_{12}$:

$$k_{2,obs} \approx k_{ue} + k_{pe}[K^c]\,[H^+]. \quad (6)$$

In Eqn. 6, k_{pe} corresponds to the rate coefficient for oxygen exchange that is enhanced by protonation of the μ_2-OH site, k_{ue} is the rate coefficient for the unenhanced pathway (i.e., uncatalyzed bridge dissociation), $[H^+]$ is the dissolved proton concentration, and K^c is the conditional equilibrium constant for protonating a μ_2-OH bridge to form a bridging water molecule:

Table 3. Structural data for Al_{13}, $GaAl_{12}$, and $GeAl_{12}$ selenate or sulfate crystals.

	Bond length (Å)			
Moiety	M = Al (III)	M = Ga(III)	M = Ge(IV)	Structural site
M_T-O	1.831 (4)	1.879 (5)	1.809	μ_4-O
Al_o-O	2.026 (4)	2.009 (6)	2.103	μ_4-O
Al_o-O	1.857 (6)	1.852 (6)	1.843 to 1.854	μ_2-OH[a]
Al_o-O	1.857 (6)	1.869 (7)	1.869 to 1.841	μ_2-OH[b]
Al_o-O	1.961 (4)	1.962 (6)	1.928	η-OH_2 (bound water)

The subscript abbreviations are T = tetrahedral, O = octahedral. The standard deviation for each bond parameter, when available, is given in parentheses and corresponds to the last place in the value. Data for Al_{13} and $GaAl_{12}$ are from Parker et al. (1997), and data for the $GeAl_{12}$ are from Lee et al. (2001). A range of values is given for the μ_2-OH^a and μ_2-OH^b sites in the $GeAl_{12}$ molecule because two crystallographically distinct octahedral aluminum sites appear in the structure of this crystal, but not in the Al_{13} or $GaAl_{12}$ salts.

$$\mu_2-OH + H^+ = \mu_2-OH_2^+; \qquad K^c = \frac{[\mu-OH_2^+]}{[H^+]\cdot[\mu_2-OH]} \tag{7}$$

at our experimental conditions. We assume that a single microscopic equilibrium constant is valid for all 12 μ_2-OH sites of a single type. This assumption may not be appropriate, in part because of the crystallographic splitting observed in the solid state, but values of K^c are unknown in any case. Substitution of Eqn. 7 into Eqn. 6 and differentiation with respect to $1/T$ (see Casey and Sposito, 1992) yields

$$E_{obs} = X_{ue}\cdot E_{ue} + X_{pe}\cdot[\Delta H^c + E_{pe}], \tag{8}$$

where E_{obs} is the Arrhenius activation energy derived by plotting $\ln(k_{2,obs})$ as a function of $1/T$ (Fig. 7), E_{ue} is the activation energy for oxygen exchange via the unenhanced pathway, E_{pe} is the activation energy for exchange via a proton-enhanced pathway, and ΔH^c is the conditional enthalpy of protonation that is derived from the temperature dependence of K^c. The factors X_{ue} and X_{pe} correspond to the fraction of the oxygen exchanges that proceeds via the unenhanced and proton-enhanced pathway, respectively: $X_{ue} = k_{ue}/k_{ue} + k_{pe}\cdot K^c\cdot[H^+]$, $X_{pe} = k_{pe}\cdot K^c\cdot[H^+]/k_{ue} + k_{pe}\cdot K^c\cdot[H^+]$, and $X_{pe} = 1 - X_{ue}$.

The E_{obs} value for oxygen exchange at the measurable μ_2-OH site in the $GeAl_{12}$ molecule is significantly smaller ($E_{obs} = 82\ [\pm 2]$ kJ · mol^{-1}, and $E_{obs} \approx \Delta H^{\ddagger}$) than corresponding values the Al_{13} and $GaAl_{12}$ (Fig. 7) because its $E_{pe} \ll E_{ue}$. The activation parameters for exchange of the less reactive hydroxyl bridge in the Al_{13} and $GaAl_{12}$ molecules are $\Delta H_2^{\ddagger} = 104\ (\pm 20)$ kJ mol^{-1} and $\Delta H_2^{\ddagger} = 125\ (\pm 4)$ kJ mol^{-1}, respectively. By analogy with the Al_{13} and $GaAl_{12}$ molecules, for which rates of oxygen exchange do not depend on pH, the values of E_{ue} for the observable site in the $GeAl_{12}$ molecule are probably near or over 100 kJ · mol^{-1}. Given the high positive charge of the $GeAl_{12}$ molecules, it is likely that ΔH^c is positive, which means that the sum $\Delta H^c + E_{pe}$ in Eqn. 8 is probably quite small.

4.2. Mechanisms of Reaction

Both pH-dependent and pH-independent mechanisms for oxygen exchange at a μ_2-OH site can involve protonation so that the exchanging moiety is a neutral water molecule. For the reaction via the pH-independent pathway, the most reasonable mechanism involves transfer of a proton from a position internal to the molecule to the μ_2-OH site, forming a bridging water molecule: μ_2-OH_2^+. This site exchanges with bulk solution and then back-transfers the proton to the original position in the molecule, which is probably a bound water molecule. A similar mechanism is likely for the proton-enhanced pathway, although the proton transfers from the solution phase to the μ_2-OH, yielding a first-order dependence of rate on $[H^+]$.

4.3. Reactivity Trends

The three molecules Al_{13}, $GaAl_{12}$, and $GeAl_{12}$ differ dramatically in reactivity (Fig. 7), even though the central site of metal substitution is three bonds away from the oxygens that exchange with bulk solution. Using rates of exchange of bridging hydroxyl oxygens as a guide, the general order of lability of these molecules is $GeAl_{12} > Al_{13} \gg GaAl_{12}$. The causes of these large differences in reactivity are not yet clear, but explanations must address propagation of structural and/or electronic effects of bonding between the central metal and the μ_4-O, because these changes are the most conspicuous difference in the molecules. The changes in bond lengths and angles at either the μ_2-OH sites or the η-OH_2 groups are not significant across the series (Table 3).

Misfit of the tetrahedral metal into the molecule appears to be important. For example, the Al_T-O distances in the Al_{13} molecule (1.831 Å, Table 3) are intermediate between the distances observed in oxide phases for aluminum coordinated to four oxygens, such as κ-Al_2O_3 (1.77 Å for κ-Al_2O_3; Table 4), and aluminum in octahedral coordination. The Ge(IV) metal has an identical ionic radius as Al(III) and a similar bond length to oxygens in tetrahedral (1.751 Å) and octahedral (1.87 to 1.91 Å) coordination to oxygens. In comparison, the Ge_T-O bond length in the $GeAl_{12}$ molecule is 1.809 Å, longer than Ge_TO bonds in other oxide minerals. Thus, Ge(IV) is as poorly fit into the M_T sites of the $GeAl_{12}$ ε-Keggin structure as Al(III) is in M_T sites of the Al_{13} molecule. The anomalous long M_T-O distances suggest that these molecules may be significantly strained, which may correlate with the high reactivity.

In contrast, the $GaAl_{12}$ molecule is the least labile among all of the ε-Keggin molecules that we have studied, and the Ga(III) metal fits easily into the M_T site of the ε-Keggin structure (Fig. 1). The Ga_T-O distances in the $GaAl_{12}$ molecule (1.88 Å) are similar to those observed other solids (1.83 to 1.86 Å, Table 4) but much different than Ga_o-O distances (1.935 to 2.074 Å).

Table 4. Bond lengths in oxides.

Site	d(M-O) Å	Phase	Source
Ge^{IV}	1.751 (4)	GeO_2; quartz structure	Yoshiasa et al. (1999)
Ge^{VI}	1.866 to 1.914	GeO_2; rutile structure	Yoshiasa et al. (1999)
Al^{IV}	1.77	κ-Al_2O_3	Ollivier et al. (1997)
Al^{VI}	1.911	κ-Al_2O_3	Ollivier et al. (1997)
	1.955	κAl_2O_3	Ollivier et al. (1997)
	1.950	κAl_2O_3	Ollivier et al. (1997)
Al^{IV}	1.777	γ-Al_2O_3	Zhou and Snyder (1991)
Al^{IV}	1.761	$Y_3Al_5O_{12}$ garnet	Euler and Bruce (1965)
Al^{VI}	1.941, 2.040	γ-Al_2O_3	Zhou and Snyder (1991)
Al^{VI}	1.937	$Y_3Al_5O_{12}$ garnet	Euler and Bruce (1965)
Al^{VI}	1.868 to 1.954	Aluminum (hydr)oxides	Smyth and Bish (1988)
Ga^{IV}	1.849	$Y_3Ga_5O_{12}$ garnet	Euler and Bruce (1965)
Ga^{IV}	1.837 to 1.863	β-Ga_2O_3	Aahman et al. (1996)
Ga^{VI}	1.995	$Y_3Ga_5O_{12}$ garnet	Euler and Bruce (1965)
Ga^{VI}	1.935 to 2.074	β-Ga_2O_3	Aahman et al. (1996)

Although these results are qualitative, they can be quantified via molecular orbital calculations that assess the amount of strain energy entered into the ε-Keggin structures by each metal substitution. The resulting strain energy, we suggest, would correlate with the rate coefficients for exchange, particularly if the strain energy in the reactive bonds is calculable; it may lead to a predictive model.

4.4. Significance to Geochemistry

Research on these small nanoclusters achieves several goals for Earth scientists. First, it provides molecular models for structural sites at the surfaces of aluminum (hydr)oxide solids in water and allows rates to be constrained for the key oxygen sites. Reactions can be followed at individual oxygens in these molecules, and we have documented both similarities and enormous differences in reactivities that could not have been anticipated from bulk studies of metal-oxide solids in water.

Second, these results provide clear test cases for models that predict rates of molecular reactions in aqueous geochemistry. A model that derives quantitative information about reaction rates from transition states in mineral dissolution, for example, must also be able to account for the extraordinary differences in rates of oxygen exchange within a single ε-Keggin (e.g., Al_{13}), among the set of substituted polyoxocations (Al_{13}, $GaAl_{12}$, and $GeAl_{12}$), and between the various Al(III) monomers (Table 2). These reaction rates are well constrained.

The importance of this work is clear when one considers the ubiquity of aluminum (hydr)oxide solids in the shallow Earth and the role that they play in our daily lives. Aluminum hydroxide solids account for much of the reactive properties of soils (Huang, 1988) and metal cycling in streams (e.g., Yu and Heo, 2001) but are also used in cosmetics (Fitzgerald and Rosenberg, 1999), foods (Yokel and McNamara, 2001), as reagents for eliminating pollutants (e.g., Lothenbach et al., 1997; Badora et al., 1998), and in vaccines and medicines (Seeber et al., 1991; Gupta, 1998).

5. CONCLUSIONS

The $GeAl_{12}$ molecule is the third ε-Keggin-like aluminum molecule for which we have determined rates of oxygen exchange. The major difference among the Al_{13}, $GaAl_{12}$, and $GeAl_{12}$ molecules is the metal in the central tetrahedral position in the molecule, which is three bonds away from the exchanging oxygens. Although the changes in <Al-O> bond lengths at the exchanging sites are relatively small, we observe large differences in reactivities among the three ε-Keggin-like molecules. Extrapolated to 298 K, the observed rates of exchange of μ_2-OH sites in these molecules span a factor of $\sim 10^5$ and are probably much larger because the most reactive set of μ_2-OH sites in the $GeAl_{12}$ molecule exchanges too quickly for us to measure using our current apparatus. The less labile set of μ_2-OH sites reacts at rates that are at least $\approx$40 and $\approx$1550 times more rapid than the corresponding μ_2-OH sites in the Al_{13} and $GaAl_{12}$ molecules, respectively. We cannot yet assign these reactive and less reactive μ_2-OH sites to the structurally distinct μ_2-OH^a and μ_2-OH^b sites in the ε-Keggin structure, but the difference arises from the relative ease of breaking bonds within, and between, the Al_3O_6 trimeric groups. We suspect that the slowly reacting μ_2-OH are within the trimers (μ_2-OH^6 in Fig. 1).

In contrast, the rate coefficients for exchange of the 12 bound water molecules are broadly similar among the three molecules and differ by a factor of $\sim$6. As with the Al_{13} and $GaAl_{12}$ molecules, we find no evidence that the μ_4-O site exchanges with bulk solution, except under conditions in which the molecule is at least partially dissociating and reforming, such as after the addition of a strong acid.

Acknowledgments—The authors thank two anonymous referees for carefully reading and improving the manuscript. Support for this research was from the U.S. National Science Foundation (NSF) via grant EAR 98-14152 and from the U.S. Department of Energy via grant DE-FG03-96ER14629. The NMR spectrometers were purchased using grants from the National Institutes of Health (grant 1S10-RR04795) and the NSF (grant BBS88-094739), and we also acknowledge the Keck Foundation for support of the solid-state NMR center at the University of California, Davis.

Associate editor: D. J. Wesolowski

REFERENCES

Aahman J., Svensson G., and Albertsson J. (1996) A reinvestigation of β-gallium oxide. *Acta Crystallogr. C, Cryst. Struct. Comm.* **C52,** 1336–1338.

Badora A., Furrer G., Grunwald A., and Schulin R. (1998) Immobili-

zation of zinc and cadmium in polluted soils by polynuclear Al-13 and Al-montmorillonite. *J. Soil Contam.* **7,** 573–588.

Casey W. H. and Sposito G. (1992) On the temperature dependence of mineral dissolution rates. *Geochim. Cosmochim. Acta* **56,** 3825–3830.

Casey W. H. and Phillips B. L. (2000) The kinetics of oxygen exchange between sites in the $GaO_4Al_{12}(OH)_{24}(H_2O)_{12}^{7+}$(aq) molecule and aqueous solution. *Geochim. Cosmochim. Acta* **65,** 705–714.

Casey W. H., Phillips B. L., Nordin J. P., and Sullivan D. J. (1998) The rates of exchange of water molecules from Al(III)-methylmalonate complexes: The effect of chelate ring size. *Geochim. Cosmochim. Acta* **62,** 2789–2797.

Casey W. H., Phillips B. L., Karlsson M., Nordin S., Nordin J. P., Sullivan D. J., and Neugebauer-Crawford S. (2000) Rates and mechanisms of oxygen exchanges between sites in the $AlO_4Al_{12}(OH)_{24}(H_2O)_{12}^{7+}$(aq) complex and water: Implications for mineral surface chemistry. *Geochim. Cosmochim. Acta* **64,** 2951–2964.

Cavanagh J., Fairbrother W. J., Palmer A. G., and Skelton N. J. (1996) *Protein NMR Spectroscopy: Principles and Practice*. Academic Press, San Diego, CA.

Cotton F. A., Wilkinson G., Murillo C. A., and Bochmann M. (1999) *Advanced Inorganic Chemistry*, 6th ed. John Wiley, New York.

Euler F. and Bruce J. A. (1965) Oxygen coordinates of compounds with garnet structure. *Acta Crystal.* **19,** 971–978.

Fitzgerald J. J. and Rosenberg A. H. (1999) Chemistry of aluminum chlorohydrate and activated aluminum chlorohydrates. In *Antiperspirants and Deodorants* (ed. K. Laden), pp. 83–136. Marcel Dekker, New York.

Furrer G., Ludwig C., and Schindler P. W. (1992) On the chemistry of the Keggin Al-13 polymer. *J. Coll. Interf. Sci.* **149,** 56–67.

Gupta R. K. (1998) Aluminum compounds as vaccine adjuvants. *Adv. Drug Deliv. Rev.* **32,** 155–172.

Huang P. M. (1988) Ionic factors affecting aluminum transformations and the impact on soil and environmental sciences. *Adv. Soil Sci.* **8,** 1–76.

Hugi-Cleary D., Helm L., and Merbach A. E. (1985) Variable temperature and variable pressure ^{17}O NMR study of water exchange of hexaquaaluminum(III). *Helv. Chim. Acta* **68,** 545–554.

Lee A. P., Phillips B. L., Olmstead M. M., and Casey W. H. (2001). Synthesis and characterization of the $GeO_4Al_{12}(OH)_{24}(OH_2)_{12}^{8+}$ polyoxocation. *Inorg. Chem.* **40,** 4585–4587.

Lothenbach B., Furrer G., and Schulin R. (1997) Immobilization of heavy metals by polynuclear aluminium and montmorillonite compounds. *Environ. Sci. Tech.* **31,** 1452–1462.

Nordin J. P., Sullivan D. J., Phillips B. L., and Casey W. H. (1998) An ^{17}O-NMR study of the exchange of water on $AlOH(H_2O)_5^{2+}$(aq). *Inorg. Chem.* **37,** 4760–4763.

Ollivier B., Retoux R., Lacorre P., Massiot D., and Ferey G. (1997) Crystal structure of kappa-alumina: An X-ray powder diffraction, TEM and NMR study. *J. Mat. Chem.* **7,** 1049–1056.

Parker W. O., Jr., Millini R., and Kiricsi I. (1997) Metal substitution in Keggin-type tridecameric aluminum-oxo-hydroxy clusters. *Inorg. Chem.* **36,** 571–576.

Phillips B. L., Neugebauer-Crawford S., and Casey W. H. (1997b) Rate of water exchange between $Al(C_2O_4)(H_2O)_4^+$(aq) complexes and aqueous solution determined by ^{17}O-NMR spectroscopy. *Geochim. Cosmochim. Acta* **61,** 4965–4973.

Phillips B. L., Casey W. H., and Karlsson M. (2000). Bonding and reactivity at oxide mineral surfaces from model aqueous complexes. *Nature* **404,** 379–382.

Seeber S. J., White J. L., and Hem S. L. (1991) Solubilization of aluminum-containing adjuvants by constituents of interstitial fluid. *J. Perenteral Sci. Tech.* **45,** 156–159.

Smyth J. R. and Bish D. L. (1988) *Crystal Structures and Cation Sites of the Rock-Forming Minerals*. Allen and Unwin, London.

Springborg J. (1988) Hydroxo-bridged complexes of chromium(III), cobalt(III), rhodium(III) and iridium(III). *Adv. Inorg. Chem.* **32,** 55–169.

Sullivan D. J., Nordin J. P., Phillips B. L., and Casey W. H. (1999) The rates of water exchange in Al(III)-salicylate and Al(III)-sulfosalicylate complexes. *Geochim. Cosmochim. Acta* **63,** 1471–1480.

Swift T. J. and Connick R. E. (1962) NMR relaxation mechanisms of ^{17}O in aqueous solutions of paramagnetic cations and the lifetime of water molecules in the first coordination sphere. *J. Chem. Phys.* **37,** 307–320.

Thompson A. R., Kunwar A. C., Gutowsky H. S., and Oldfield E. (1987) Oxygen-17 and aluminum-27 nuclear magnetic resonance spectroscopic investigations of aluminum(III) hydrolysis products. *J. Chem. Soc. Dalton Trans.* **1987,** 2317–2322.

Yokel R. A. and McNamara P. J. (2001). Aluminum toxicokinetics: An updated minireview. *Pharmacol. Toxicol.* **88,** 159–167.

Yoshiasa A., Tamura T., Kamishima O., Murai K.-I., Ogata K., and Mori H. (1999) Local structure and mean-square relative displacement in SiO_2 and GeO_2 polymorphs. *J. Synchrotron Rad.* **6,** 1051–1058.

Yu J. Y. and Heo B. (2001). Dilution and removal of dissolved metals from acid mine drainage along Imgok Creek, Korea. *Appl. Geochem.* **16,** 1041–1053.

Yu P., Phillips B. L., and Casey W. H. (2001). Water exchange in fluoroaluminate complexes in aqueous solution: A variable temperature multinuclear NMR study. *Inorg. Chem.* **40,** 4750–4754.

Zhou R.-S. and Snyder R. L. (1991) Structures and transformation mechanisms of the η, γ and θ transition aluminas. *Acta Cryst.* **B47,** 617–630.